Monitoring soybean growth and yield due to topographic variation using UAV-based remote sensing

Jianfeng Zhou [1], Aijing Feng [1], Kenneth Sudduth [2]

[1] Division of Food Systems and Bioengineering, University of Missouri, Columbia, MO 65211, USA

[2] USDA-ARS, Columbia, MO 65211, USA

A paper from the Proceedings of the
14th International Conference on Precision Agriculture
June 24 – June 27, 2018
Montreal, Quebec, Canada

Abstract. *Remote sensing has been used as an important tool in precision agriculture. With the development of unmanned aerial vehicle (UAV) technology, collection of high-resolution site-specific field data becomes promising. Field topography affects spatial variation in soil organic carbon, nitrogen and water content, which ultimately affect crop performance. To improve crop production and reduce inputs to the field, it is critical to collect site-specific information in a real-time manner and at a large scale. The goal of this study was to evaluate the feasibility of a remote sensing system based on a UAV and imaging sensors to quantify the influence of topographic variables on apparent soil electrical conductivity (ECa) and plant performance. The experiment was conducted in 6.2 ha area within a 20-ha research soybean field with varying topography. Geo-referenced ECa data were collected before planting soybean in 2017. Geo-referenced crop yield was measured using a yield monitor system in 2016 and 2017. A RGB camera and a multispectral camera were used to take images on the field at four critical times during soybean growth in 2017. The UAV system was flying at an altitude of 100 m or 50 m above ground level with an image overlap > 70%. The image data were processed to generate geo-referenced orthophotos and a digital surface model (DSM) which was used to develop a digital elevation model (DEM). Results showed that image-based elevation represented 95% of the variability in elevation as measured by a GPS system. Results show that the relationships of field topography, i.e. elevation and slope, to soil ECa and crop were significant. Field regions with the lowest elevation had significantly lower yield and the lowest normalized difference vegetation index (NDVI) values, indicating a negative effect on crop development. Meanwhile, field slope also showed significant relationships to crop development, with significantly lower NDVI and crop yield in regions having the highest slope. The study showed that it was possible to use UAV-based remote sensing for monitoring crop growth and yield differences due to topographic variation.*

Keywords. *UAV, remote sensing, field topography, soil variation, soybean production.*

Introduction

Field topography, such as elevation, slope and flow accumulation, has an important impact on spatial variation of soil organic carbon, nitrogen and water content, which ultimately affect crop growth and yield. Among field topographic attributes, terrain slope affects soil moisture content and transpiration rate because that soil moisture became spatially organized across the hillslope during a short transition between the wet and dry state (Tromp-van Meerveld and McDonnell, 2006). Lower elevation, concave slope regions usually have more water content (Zhu et al., 2015). Crop yield is affected by topography due to yield dependence on soil. Spatial variability of maize yield was found to correspond to profile curvature and slope (Zhu et al., 2015). Topography has more impact on crop yield in dry regions and drought periods due to its significant influence on soil water content (Kumhálová et al., 2011; Muñoz et al., 2014). Therefore, it is critical to monitor crop growth in different growth stages and quantify the relationship of field topography to yield to improve crop production and manage crops efficiently.

Field topography can be mapped using a RTK-GPS (Real Time Kinematic Global Positioning System) operated by hand (Kumhálová et al., 2008) or mounted on a combine (Kumhálová et al., 2011). However, the number of sampling points was limited, and the digital surface model (DSM) derived using spatial interpolation (e.g. nearest-neighbor interpolation, bilinear interpolation cubic convolution and kriging regression) might result in large measurement errors (Kumhálová et al., 2011; Wu et al., 2008). High-resolution topography data can be obtained by airborne Light Detection and Ranging (LiDAR) (Muñoz et al., 2014); however, high-resolution LiDAR is expensive and it is not convenient to operate an airplane. With the development of UAV and imaging processing technologies, it is possible to monitor crop and field topography using a small UAV equipped with a low-cost camera. UAV, as a high-throughput tool, can fly at low altitudes with large image overlap to acquire ultra-high spatial resolution images (Turner et al., 2014). Images collected by UAV have been used to generate high-resolution DSM and orthomosaics (Yang et al. 2017).

The goal of this study was to evaluate the feasibility of a remote sensing system based on a UAV and imaging sensors to quantify the influence of topographic variables on soil ECa and crop growth in a soybean field. The objectives were: 1) to map the elevation and slope of an experimental field using the UAV imaging system; 2) to evaluate the effect of field topography on soil ECa and soybean growth.

Materials and Methods

Experimental Field and Ground Data Collection

This study was conducted on a soybean field at the Rocheford Turkey Research Farm of the University of Missouri (MU) located in Boone County, MO, USA (38°58'29.0" N 92°11'14.3" W). The field was about 20 ha in total, from which a region of 270 m × 235 m (about 6.3 ha) was selected to collect data (marked in Fig. 1a with dashed lines). From Fig. 1a, it can be seen that a lake is located in the corner of the field, where the elevation is the lowest. The elevation of the selected region is from 260 m to 267 m above mean sea level (MSL) which results in rainfall flowing to the lake from surrounding areas. The apparent soil electrical conductivity (ECa) of the farm was measured prior to planting of soybean in the spring 2017 using a soil ECa mapping system (model: 3100, Veris Technologies, Salina, KS) integrated with a GPS system to record the geo-information of each measurement. In this study, 2927 soil ECa sample points were obtained from the selected region. Prior to planting, burndown herbicides (2,4-D: 1.68 $kg \cdot ha^{-1}$ and Roundup: 2.24 $kg \cdot ha^{-1}$) were applied for control of winter annual broadleaf weeds. Soybean (MorSoy 4327, MFA Incorporated, Columbia, MO) was planted at a population of 56,660 seeds per ha on May 31, 2017 using a 6-row soybean planter (Kinze Manufacturing, Williamsburg, Iowa, USA). Pre-emergent herbicides (Roundup: 2.24 $kg \cdot ha^{-1}$ and Fierce XLT 2.62 $kg \cdot ha^{-1}$) were applied at the same day of planting and post-emergent herbicides (Roundup: 2.24 $kg \cdot ha^{-1}$, Select Max

1.12 kg·ha^{-1} and Warrant 1.68 kg·ha^{-1}) were applied on July 2, 2017 (32 days after planting). Soybeans were harvested on October 15, 2017 using a combine harvester (Case IH, Racine, WI) equipped with an Ag Leader Insight (Ag Leader Technology, Ames, IA) yield monitor system, which was able to record geo-referenced yield data points every one second. After harvesting, yield data were "cleaned" with the Yield Editor software (Sudduth et al., 2012) to remove abnormal data points and shift GPS coordinates to the center of harvesting rows. In this study, 2089 yield data points were collected in the selected region. Precipitation data was acquired from a nearby weather station (MU Bradford Research Center), and the accumulative precipitation and temperature in the year 2017 is shown in Fig. 1b.

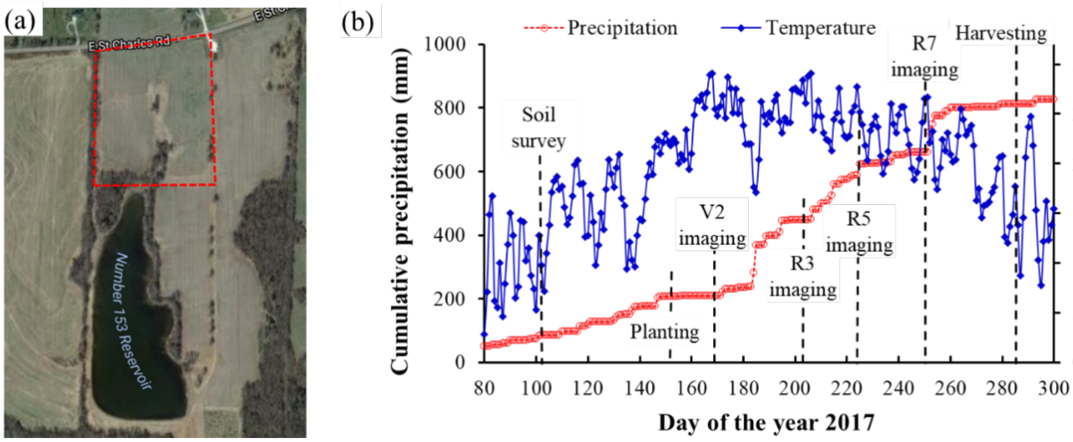

Fig. 1. (a) Experimental field. Red dashed trapezoid shows the location of the selected region. A lake is located in bottom-left corner of the field. (b) Accumulative precipitation and daily air temperature in 2017.

UAV-based Image Data Acquisition

A UAV-based remote sensing system was developed by integrating a UAV platform (Dji Matrice 600 Pro, DJI, China) with an RGB camera (HERO 5, GoPro) and a customized multispectral camera using a Canon PowerShot ELPH130HS (Canon U.S.A. Inc.) by a company (LDP LLC, Carlstadt, NJ, USA). The specifications of the cameras are listed in Table 1. The RGB camera was set to capture still images at a rate of two frames per second (fps) and images were saved on an on-board SD card. An open-source third-party firmware (CHDK, http://chdk.wikia.com) was used to control the multispectral camera to allow automatic snapshotting at an interval of about 2.5 s per image and saving images on its on-board SD card.

Table 1. Parameter of Cameras used in this study.

Camera name	Model	Spectrum of each channel	Snapshot rate (s/image)	Resolution (pixel)	Spatial resolution
Multispectral camera	ELPH110HS	NIR (680-800), R (550-720), G (500-620)	2.5	4608 × 3456	1.56 cm/pixel
RGB camera	GoPro Hero 5	R-G-B	1	4000×3000	2.6 cm/pixel

Flight of the UAV was controlled using a UAV ground control app (Autopilot, Hangar Technology, Austin, TX, USA), which allows planning flight path, setting way-points, flight speed and flight altitude (above ground level). Before each flight, flight path and speed were planned properly according to flight height and a minimum overlap requirement (>60% in forward and sideward directions). After each flight, geo-information of the UAV on-board GPS system and images were downloaded for further processing. Image data were collected at four soybean growth stages described by Fehr & Caviness (1977), as shown in Table 2.

Table 2. Field activities and data collection time line

Field activity (growth stages)	Date	Flight height (m, AGL)
Soil survey	Feb 16-17	--
Imaging	April 11	100
Planting	May 31	--
Imaging (V2)	June 20	100
Imaging (R3)	July 24	100
Imaging (R5)	August 13	100
Imaging (R7)	September 07	50
Harvest	October 15	--

Image Pre-processing

Sequential images from the cameras were stitched using Agisoft PhotoScan Pro (Version 1.4.1, Agisoft LLC., Russia), which was able to generate dense point cloud data based on the structure-from-motion (SfM) method (Glendell et al., 2017). GPS information obtained from the UAV platform was manually matched with every image based on their time stamps. The geo-referenced images were uploaded to the software to generate dense point cloud data, orthomosaic images and a digital elevation model (DEM). The DEM map was generated using RGB images acquired on April 11, 2017, which had the higher overlap and were expected to provide higher DEM accuracy because they were obtained before the crop was planted (Torres-Sánchez et al., 2017).

In this study, an image feature-based geo-registration method was developed to register coordinates in images and GPS coordinates associated with the yield mapping and soil survey. Five ground control points (GCPs) were distributed in the selected region and their GPS coordinates were recorded using the GPS on the UAV. The coordinates of the GCPs were manually extracted from the orthomosaic images, and the GPS coordinates and image coordinates of the GCPs were used to calculate conversion coefficients that registered geo-referenced data of ECa and yield data with image coordinates, as shown in Eq. 1.

$$\begin{cases} k_x = \frac{|x_{Gi}-x_{Gj}|}{|x_{Ii}-x_{Ij}|} \\ k_y = \frac{|y_{Gi}-y_{Gj}|}{|y_{Ii}-y_{Ij}|} \end{cases}, i, j = 1, 2, 3, 4, 5, i \neq j \quad (1)$$

where, k_x and k_y are the conversion coefficients in x and y direction respectively, (x_{Gi}, y_{Gi}), (x_{Ii}, y_{Ii}) and (x_{Gj}, y_{Gj}), (x_{Ij}, y_{Ij}) are the GPS coordinate and image coordinate of the i^{th} and the j^{th} GCP, respectively. The conversion coefficients were used to convert all the GPS coordinate points to image coordinate points using Eq. 2.

$$\begin{cases} x_{GI} = x_{Gi} \times k_x + x_0 \\ y_{GI} = y_{Gi} \times k_y + y_0 \end{cases}, i = 1, 2, 3, 4, 5 \quad (2)$$

where, (x_{GI}, y_{GI}) is the image coordinate converted from a GPS coordinate, (x_{Gi}, y_{Gi}) is a GPS coordinate in the geo-referenced ECa or yield data, and (x_0, y_0) is the image coordinate of a GCP. Fig. 2 shows the geo-referenced ECa and yield data that were plotted on an orthomosaic image collected on July 24, 2017. As it is shown in the figure, tracks of soil and yield data were not aligned with each other. To align geo-referenced data points of ECa (soil) and yield with image coordinates, data points of yield (fewer in number) and ECa were gathered based on their minimum Euclidean distance, i.e. the soil data points were assigned to their nearest yield data points.

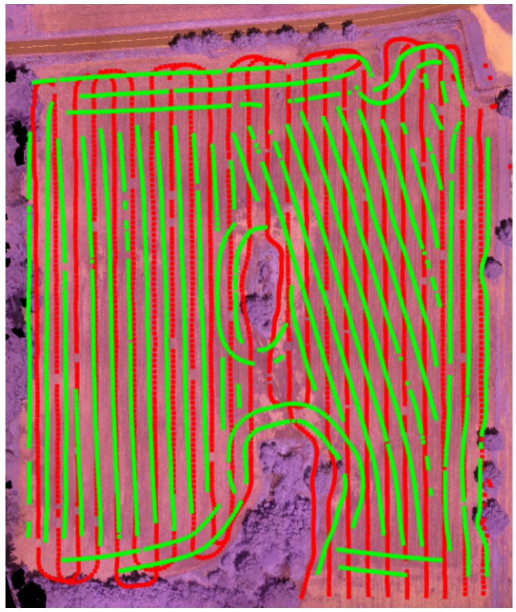

Fig. 2. Registered geo-referenced soil and yield data plotted on an orthomosaic image. The red line indicates the route of ECa soil survey and the green line indicates the route of harvesting

Topographic Attributes and NDVI Extraction

Elevation of the selected field region was extracted from the DEM map. The accuracy of the image-based elevation was evaluation by comparing with the elevation obtained with a RTK-GPS system (Geo 7X, Trimble, Sunnyvale, CA) that traversed the field on the same day and on approximately the same transects as the ECa sensor (Fig. 2). The terrain (surface) slope of the field, representing the rate of elevation change for each digital elevation model cell, was calculated based on the DEM map. For raster slope calculation, a moving window was used to perform this process in *x* and *y* direction using the planar slope algorithm developed by Burrough et al. (1998). In this study, the spatial resolution of the DEM was 5.2 cm per pixel as determined by the field of view of the camera and the UAV flight attitude (100 m AGL). To achieve a reasonable scale for the calculation of field slope, a 100-pixel moving window, equivalent of about a 5-m^2 area, was used to calculate the slope at each point. In addition, NDVI maps for the selected test regions were calculated from multispectral images acquired at the four growth stages using Eq. 3.

$$NDVI = \frac{NIR-Red}{NIR+Red} \qquad (3)$$

The numbers of geo-referenced data points of ECa and yield were much smaller than the data obtained from the images (elevation, slope and NDVI). Therefore, image-based features were resampled by calculating the mean of pixel values in a rectangular area (80 × 60 pixels, equivalent to 12.8 m^2) centered on each geo-referenced data point. A balanced data set, including all geo-referenced data and image-based data, for each image collection date was established based on the data points.

To evaluate the effect of topography (elevation and slope) on the ECa and crop variables, the data set was firstly divided into five groups (levels) based on the elevation, i.e. E1 to E5 from the lowest to the highest elevation. Then data in each elevation group were split into three sub-sets based on the slope in ascending order. A linear regression analysis was conducted to evaluate the accuracy of elevation extracted from the UAV-based DEM compared with elevation data collected by the ground-based GPS receiver. The variation in elevation, ECa, NDVIs and yield was assessed using ANOVA (‘PROC GLM’) analysis with the least square mean difference (‘LSMEANS/PDIFF’) option to compare the differences at a 0.05 level of significance. The results were used to evaluate the effect of topographic attributes on ECa, crop development and yield. All statistical analyses were conducted using SAS 9.4 software (SAS Institute, Cary, NC, USA).

Results and Discussion

Image-based DEM Map

UAV-based remote sensing provides a convenient approach to measure the variation of field elevation. The accuracy of the measurement in elevation was evaluated by comparing with the elevation measured by the RTK-GPS system. Fig. 3 illustrates the DEM model developed with images collected prior to planting, where Fig. 3(a) shows the RGB orthomosaic image of the test plot, Fig. 3(b) shows the corresponding DEM map and Fig. 3(c) shows the relationship between elevations of image- and GPS-based measurement. The result of a linear regression analysis indicated that elevation extracted from image-based DEM fitted with that of GPS well, with the coefficient of determination R^2 = 0.96 and RMSE = 0.5 m. Comparing to GPS-based elevation, the image-based DEM may provide a fast approach for measuring the elevation of a field with more detail (high-resolution data). The developed DEM map might be used to monitor crop growth and calculate various topographic attributes for site-specific management.

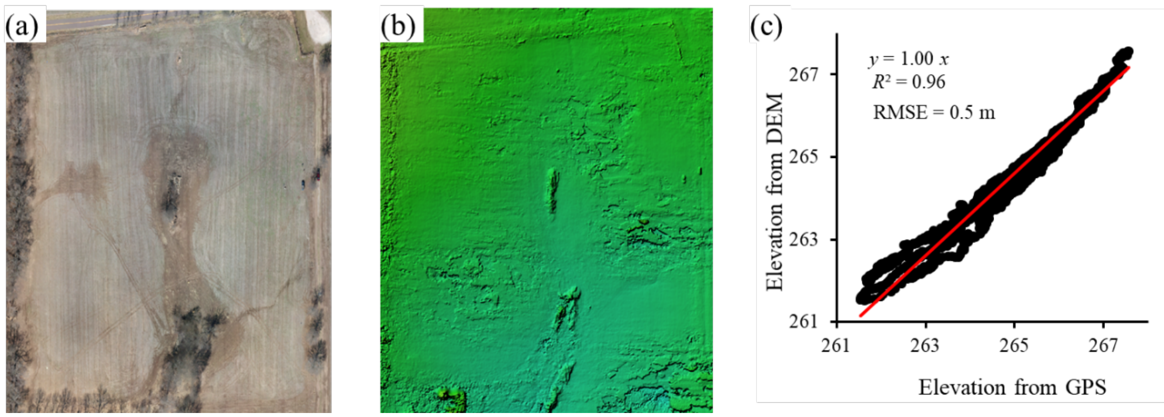

Fig. 3. Elevation measured with imaging method. (a) RGB orthomosaic image of test field taken prior to planting. (b) DEM map generated based on images and (c) fitness between elevations measured by imaging method and a RTK GPS system.

Effect of Topographic Variation on ECa and Yield

Topographic attributes derived from the DEM, including elevation and terrain slope, were used to evaluate the effect of topography on ECa and crop development. The least squares means (lsm) of elevation in the five ranges (E1 – E5 as shown in Table 3) were significantly different (p < 0.001) at 5% significance level based on an ANOVA analysis. The data in each elevation level were sorted in ascending order by the terrain slope and then evenly split into three sets (Table 3). The relationship of crop NDVIs in different growth stages and yield in 2016 and 2017 to the topographic attributes was analyzed using ANOVA and the results are shown in Fig. 4b and Fig. 4b, respectively. At the vegetative stage (V2), soybean NDVI was significantly higher in the region with lower elevation (E1) than in higher elevation levels. As shown in Fig. 1b, the accumulative precipitation was low when crop images in V2 stage were collected (21 days after planting), and no precipitation was received since planting. Since the development of the soybean root system needs sufficient water (Quach et al., 2014), crops in the low-elevation regions, where soil might have higher water content than high-elevation regions (Zhu et al., 2015), had more vegetation (higher NDVI). The lowest NDVI values, in regions with E4 level might be because of higher slopes. However, in the later crop growth stages (R3, R5 and R7), NDVI in the regions with the low elevation E1 were consistently lower among all five elevation levels (as shown in Fig. 4a). This phenomenon might be explained by the large accumulative precipitation during the later growth stages, which might have reduced the difference in soil moisture at different elevations. Meanwhile, the established root system might help the plants access more water and reduce water stress in regions of middle and high elevation. Also, heavy precipitation might cause waterlogging or flooding stress for crops in the lower regions and thereby affect crop development (Kim et al., 2015).

Table 3. Elevation and slope levels in the divided data ranges. Different lower-case letters indicated significant difference in least square means at different levels.

E1 (m)	Slope (degree)	E2 (m)	Slope (degree)	E3 (m)	Slope (degree)	E4 (m)	Slope (degree)	E5 (m)	Slope (degree)
	0.9 ± 0.2		1.3 ± 0.2		1.2 ± 0.3		1.2 ± 0.3		1.3 ± 0.4
262.4 ± 0.4 (a)	1.4 ± 0.1	263.0 ± 0.5 (b)	1.9 ± 0.2	263.8 ± 0.4 (c)	1.9 ± 0.2	264.4 ± 0.4 (d)	1.8 ± 0.2	265.4 ± 1.2 (e)	2.1 ± 0.1
	2.4 ± 1.1		3.4 ± 1.7		3.3 ± 1.4		2.7 ± 0.7		2.7 ± 0.7

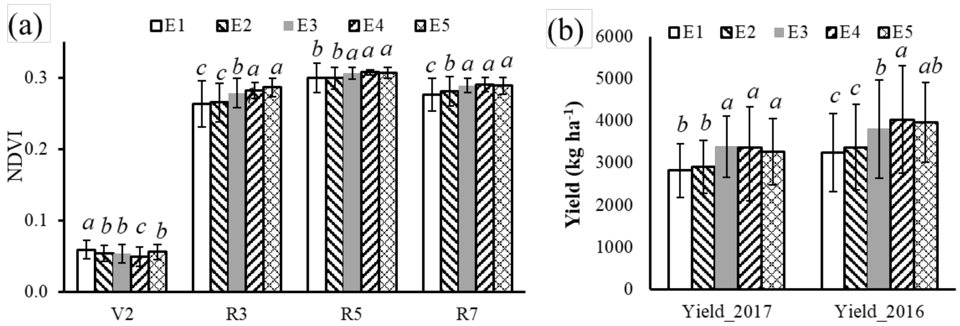

Fig. 4. Relationship of elevation to crop development and yield. (a) Response of NDVI to different elevations at four growth stages, and (b) response of crop yield to different elevations. ANOVA test was conducted to compare the least squares means of NDVI and yield in different elevation levels at four growth stages and two years, respectively. Different lower-case letters indicate a significant difference at the 5% level.

More evidence of the effect of topography on crop development can be seen in Fig. 5, which shows the variation in elevation and NDVI along one row in the field. The figure clearly shows that NDVI values were generally decreasing along with the decrease of elevation. The lower NDVI was caused by less vegetation in the region of low elevation (A2 in Fig. 5). The NDVI values might also be affected by slope of field. In marked area A1 in Fig. 5, the location with a jump in elevation showed a drop in NDVI. However, ANOVA results in Fig. 4a show no significant effect of elevation on NDVIs in the regions with higher elevation (E4-E5). Similarly, crop yield in lower elevation levels (E1 and E2) was significantly lower than those in higher elevation levels (E4 & E5) in both years (Fig. 4b).

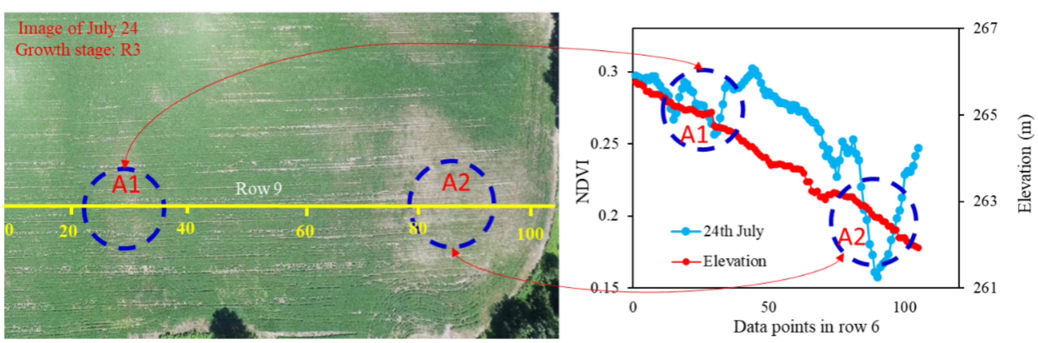

Fig. 5. Illustration of NDVI variation at different levels of elevation. Row was extracted using GPS information in yield data

The effect of terrain slope on yield and soil was also significant. Overall, yield was significantly (*p* < 0.001) higher in low-slope regions than area with steep slopes in both years, likely due to reduced soil quality from erosion in areas of steeper slopes. ANOVA results also show that the interaction effect of elevation and slope was significant on soil ECa values and soybean yield in both years ($p \leq 0.001$ at 5% significance level). As shown in Fig. 6a, soil ECa response to slope variation was significantly different in high elevation regions (E4 and E5). ECa in low-slope regions was significantly higher than in regions with steep slope. However, soil ECa in regions with lower elevation was not significantly affected by terrain slope, which was possibly due to less dynamic range in ECa values in that area. The effect of field topography on yield showed a similar pattern as those for ECa. As shown in Fig. 6b, yield in 2017 and 2016 was significantly higher at high-elevation regions (E3-E5, in 2017 or E5 in 2016 (not shown here)) with low slope (Slope1) than that with steep slopes. However, crop yield variance with slope in the low-elevation regions (E1-E2) was not significant.

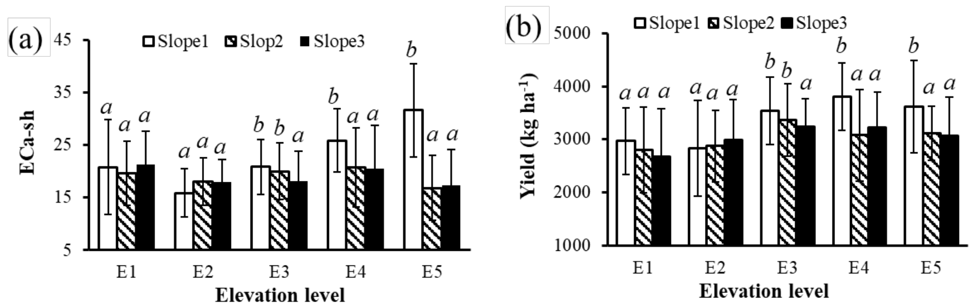

Fig. 6. Interaction effect of field elevation and slope on soil ECa and crop yield. (a) Response of soil ECa to field elevation and slope, and (b) response of yield to field elevation and slope

To understand the effect of soil ECa on yield, the least squares means of yield at different ECa levels were calculated. The ECa levels were acquired by sorting data according to ECa values in ascending order and evenly split into five levels, i.e. EC1-EC5. As shown in Fig. 7, there was a positive effect of soil ECa on yield, with areas of higher ECa consistently yielding more soybeans than areas of lower ECa in both years.

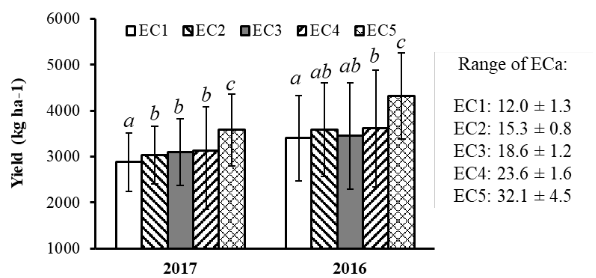

Fig. 7. Effect of soil ECa on crop yield. Statistical analysis was conducted to compare least squares means in yield due to five split levels of EC within each year separately. Different lower-case letters indicate significant differences at a 5% significance level

Summary

A UAV-based remote sensing system was evaluated for feasibility in monitoring crop development and soil and topography variation in a soybean field. A field DEM was successfully developed using images collected using a UAV platform. The accuracy of the derived elevation was evaluated by comparing with elevation from a RTK-GPS system, and analysis results showed that R^2 between these two measurements was 0.95. Results indicated that UAV-based remote sensing had potential to map the elevation of a field. The field slope map was also established based on the DEM, and used to evaluate the effect of topography on soil and crop. A multispectral camera was used to collect soybean images in four different growth stages. The derived NDVI was used to monitor the growth status of the soybean crop.

Field elevation was split into five levels to test the response of soil ECa and crop to the variation of elevation and slope. Statistical analysis indicated that elevation significantly affected crop yield, with the area with the lowest elevation yielding the least. The effect of elevation on NDVI was not consistent at different stages. Lower elevation benefited the growth of crop in an early vegetative stage, but negatively affected crop growth (less vegetation) afterward. Field slope and elevation affected crop and soil jointly. The interaction effect of elevation and slope was analyzed and it was found that slope affected soil and yield significantly in the region with high elevation, with low-slope regions yielding significantly more crop than steep slope regions. This study indicated the potential of using remote sensing in analysis of the effect of topography on crop growth and yield.

Acknowledgements

We would like to give our thanks to the University of Missouri Agricultural Experiment Station for significant help in providing the research field, preparing, and managing and harvesting crops. We would like to give our special thanks to Mr. Andrew Biggs, Mr. Joshua Reinbott and Mr. Timothy Reinbott from AES for help in managing the field and data collection. We also thank Mr. Scott Drummond for helping to pre-process geo-referenced data.

References

Burrough, P. A., & McDonell, R. A. (1998). *Principles of geographical iInformation systems* New York: Oxford University Press.

Chang, A., Jung, J., Maeda, M. M., & Landivar, J. (2017). Crop height monitoring with digital imagery from Unmanned Aerial System (UAS). *Computers and Electronics in Agriculture*, 141, 232-237.

Fehr, W. R., & Caviness, C. E. (1977). *Stages of soybean development*. Ames, IA: Iowa State University.

Glendell, M., McShane, G., Farrow, L., James, M. R., Quinton, J., Anderson, K., & Brazier, R. E. (2017). Testing the utility of structure-from-motion photogrammetry reconstructions using small unmanned aerial vehicles and ground photography to estimate the extent of upland soil erosion. *Earth Surface Processes and Landforms*, 42(12), 1860-1871.

Kim, Y. H., Hwang, S. J., Waqas, M., Khan, A. L., Lee, J. H., Lee, J. D., & Lee, I. J. (2015). Comparative analysis of endogenous hormones level in two soybean (Glycine max L.) lines differing in waterlogging tolerance. *Frontiers in Plant Science*, 6, 714-730.

Kumhálová, J., Kumhála, F., Kroulík, M., & Matějková, Š. (2011). The impact of topography on soil properties and yield and the effects of weather conditions. *Precision Agriculture*, 12(6), 813-830.

Kumhálová, J., Matejkova, S., Fifernová, M., Lipavsky, J., & Kumhála, F. (2008). Topography impact on nutrition content in soil and yield. *Plant Soil and Environment*, 54(6), 255-261.

Muñoz, J. D., Steibel, J. P., Snapp, S., & Kravchenko, A. N. (2014). Cover crop effect on corn growth and yield as influenced by topography. *Agriculture, Ecosystems & Environment*, 189, 229-239.

Quach, T. N., Tran, L. S., Valliyodan, B., Nguyen, H. T., Kumar, R., Neelakandan, A. K., Guttikonda, S. K., Sharp, R. E., & Nguyen, H. T. (2014). Functional analysis of water stress-responsive soybean GmNAC003 and GmNAC004 transcription factors in lateral root development in *arabidopsis*. *PLoS One*, 9(1): e84886.

Sudduth, K. A., Drummond, S. T., & Myers, D. B. (2012). Yield editor 2.0: software for automated removal of yield map errors. ASABE Paper No. 121338243. St. Joseph, MI: American Society of Agricultural and Biological Engineers.

Torres-Sánchez, J., López-Granados, F., Borra-Serrano, I., & Peña, J. M. (2017). Assessing UAV-collected image overlap influence on computation time and digital surface model accuracy in olive orchards. *Precision Agriculture*, 19(1), 115-133.

Tromp-van Meerveld, H., & McDonnell, J. (2006). On the interrelations between topography, soil depth, soil moisture, transpiration rates and species distribution at the hillslope scale. *Advances in Water Resources*, 29(2), 293-310.

Turner, D., Lucieer, A., Malenovský, Z., King, D. H., & Robinson, S. A. (2014). Spatial co-registration of ultra-high resolution visible, multispectral and thermal images acquired with a micro-UAV over Antarctic moss beds. *Remote Sensing*, 6(5), 4003-4024.

Wu, S., Li, J., & Huang, G. H. (2008). A study on DEM-derived primary topographic attributes for hydrologic applications: Sensitivity to elevation data resolution. *Applied Geography*, 28(3), 210-223.

Yang, G., Liu, J., Zhao, C., Li, Z., Huang, Y., Yu, H., & Yang, H. (2017). Unmanned aerial vehicle remote sensing for field-based crop phenotyping: Current status and perspectives. *Frontiers in Plant Science*, 8, 1111.

Zhu, Q., Schmidt, J. P., & Bryant, R. B. (2015). Maize (Zeamays L.) yield response to nitrogen as influenced by spatio-temporal variations of soil–water-topography dynamics. *Soil and Tillage Research*, 146, 174-183.